Electronic Structures of Transition-metal Four-co-ordinated Complexes. Part 3.† Theoretical *Ab Initio* and Ultraviolet Photoelectron Spectroscopy Study of Nickel(II), Palladium(II), and Platinum(II) Bis(*O,O'*-diethyl dithiophosphate) Square-planar Complexes‡

Enrico Ciliberto, Santo Di Bella, and Ignazio Fragalà
Dipartimento di Scienze Chimiche, University of Catania, 95125 Catania, Italy
Gaetano Granozzi
Dipartimento di Chimica Inorganica, Metallorganica ed Analitica, University of Padova, 35100 Padova, Italy
Neil A. Burton and Ian H. Hillier*
Chemistry Department, University of Manchester, Manchester M13 9PL
John Kendrick
ICI Wilton Material Research Centre, PO Box No. 90, Wilton, Middlesborough, Cleveland TS6 8JE
Martyn F. Guest
SERC Daresbury Laboratory, Warrington WA4 4AD

The electronic structures of $[Ni(dtp)_2]$, $[Pd(dtp)_2]$, and $[Pt(dtp)_2]$ [dtp = $S_2P(OEt)_2$] have been studied using pseudopotential valence-only *ab initio* methods, and He I and He II photoelectron spectroscopy. For $[Ni(dtp)_2]$ and $[Pd(dtp)_2]$, correlation and relaxation effects have been included in the calculation of the ionization energies by means of the extended two particle–hole Tamm–Dancoff method. The deviations from Koopmans' theorem were found to be considerably greater for the nickel than for the palladium complex. Consistent assignments of the photoelectron spectra have been proposed with the aid of these calculations.

Chemical and structural peculiarities of planar complexes containing MS_4 chromophores have been extensively studied.[1] In particular, metal complexes of dithiophosphoric acids form a vast and important class of compounds.[2] Among these, square-planar complexes of *O,O'*-diethyl dithiophosphate anion (dtp^-) have been extensively investigated and many studies have appeared on their chemical and electronic properties,[2b,3–5] since they offer opportunities for technological and biological applications.[2,6] Despite many theoretical studies,[3,4] their electronic structure is still not fully rationalized because different energy orderings of metal-based (m.b.) and ligand-based (l.b.) molecular orbitals (m.o.s) have been found. As a consequence different m.o. schemes have been proposed and the available results are still inconclusive.

In this context, combined gas-phase ultraviolet photoelectron (p.e.) spectroscopy and accurate quantum-mechanical calculations represent a powerful tool for obtaining details of electronic structure. On the experimental side, the intensity changes observed between He I and He II spectra can often aid the assignment of the p.e. spectra. Thus, it is generally found that bands arising from ionization of metal localized orbitals increase in intensity on going from He I to He II ionizing radiation, compared to bands associated with ligand ionization. However, it must be remembered that such simplistic arguments may not always be correct due to the possible occurrence of resonances in the p.e. spectra.[7] On the theoretical side, the calculation of ionization energies (i.e.s) of sufficient accuracy to allow an assignment of the p.e. spectra of transition-metal complexes is still far from routine. It has been recognized for some time that Koopmans' theorem is frequently inadequate due to the large difference in the reorganization energy associated with ionization of metal and ligand localized electrons which has led to the widespread use of the ΔSCF method.[8] However, such calculations ignore correlation effects which have been shown to effect the order of the ionized states of some transition-metal complexes[9] and it is difficult to calculate by this method i.e.s other than the lowest of each symmetry. The calculation of the full range of i.e.s of transition-metal complexes, including both relaxation and correlation effects, has been successfully carried out using both configuration interaction and Green's function[10] methods. We have previously used a Green's function method, in conjunction with atomic pseudo-potentials, successfully to assign the p.e. spectrum of palladium(II) acetylacetonate.[11,12] In the case of transition-metal complexes, where the one-particle picture is inadequate since there is often a large degree of electron reorganization occurring upon ionization, it is necessary to use the extended two particle–hole Tamm–Dancoff method.[13]

In this paper we report the He I and He II p.e. spectra of nickel(II), palladium(II), and platinum(II) bis(*O,O'*-diethyl dithiophosphate) $[M(dtp)_2]$ complexes. We also report the results of *ab initio* m.o. calculations, using pseudopotentials to represent the core electrons, in order to interpret these spectra, including, in the case of the nickel and palladium complexes, relaxation and correlation effects by means of the Tamm–Dancoff method. Previous studies of these complexes have been limited to their He I spectra, interpreted using qualitative bonding arguments.[4]

Experimental

The complexes were prepared according to literature methods,[2b] and were purified by recrystallization from a mixture of dichloromethane–2-propanol and by successive sublimation *in vacuo*. They gave satisfactory mass spectrometric analyses.

Photoelectron Spectroscopy.—The p.e. spectra were recorded on a PS18 Perkin-Elmer spectrometer modified by the inclusion

† Part 2 is ref. 15.
‡ Based in part on the Ph.D. thesis of S. Di Bella, University of Catania, 1986.
Non-S.I. unit employed: eV ≃ 1.60 × 10^{-19} J.

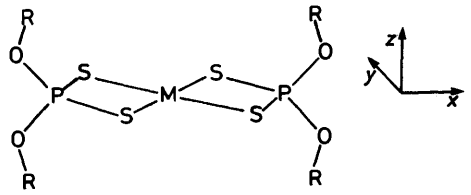

Figure 1. Schematic drawing of $[M(dtp)_2]$ complexes

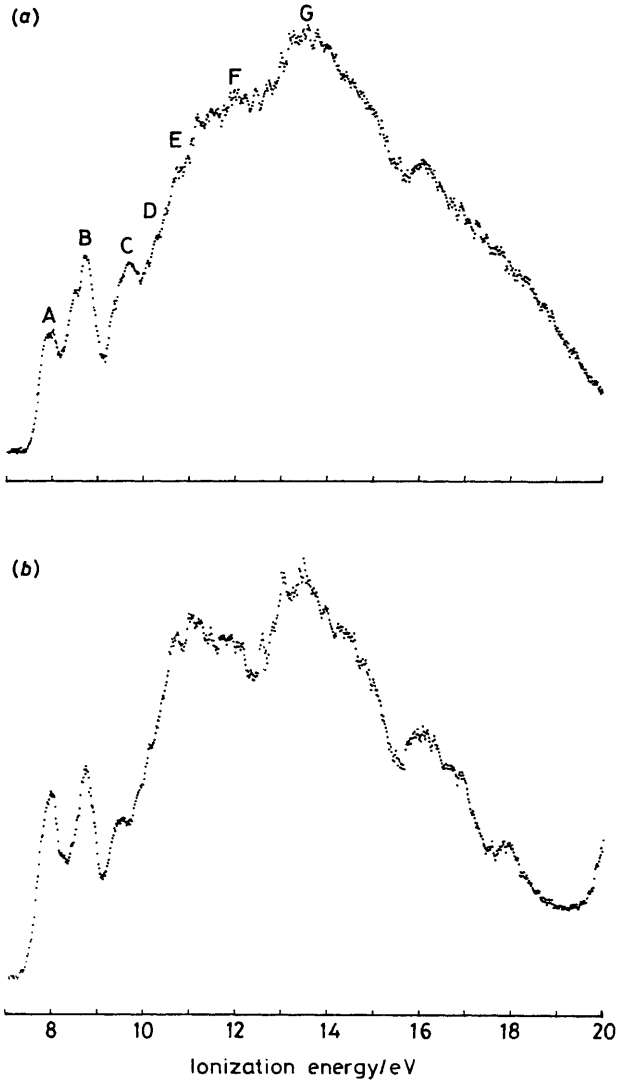

Figure 2. He I (*a*) and He II (*b*) p.e. spectra of $[Pd(dtp)_2]$

of a hollow-cathode discharge source giving high output of He II photons (Helectros Development Corp.). The operating temperatures were 130 °C for $[Ni(dtp)_2]$, 130 °C for $[Pd(dtp)_2]$, and 120 °C for $[Pt(dtp)_2]$. The spectra were accumulated in the 'multiple scan mode' with the aid of an IBM PC AT computer directly interfaced to the spectrometer. The energy scale of consecutive scans was locked to the reference values of the Ar $^2P_{\frac{3}{2}}$ and He $1s^{-1}$ self-ionization lines. Spectral resolution measured on the Ar $^2P_{\frac{3}{2}}$ lock was always better than 0.035 eV. The He II spectra were corrected only for the He IIβ 'satellite' contributions (12% on reference nitrogen spectrum).

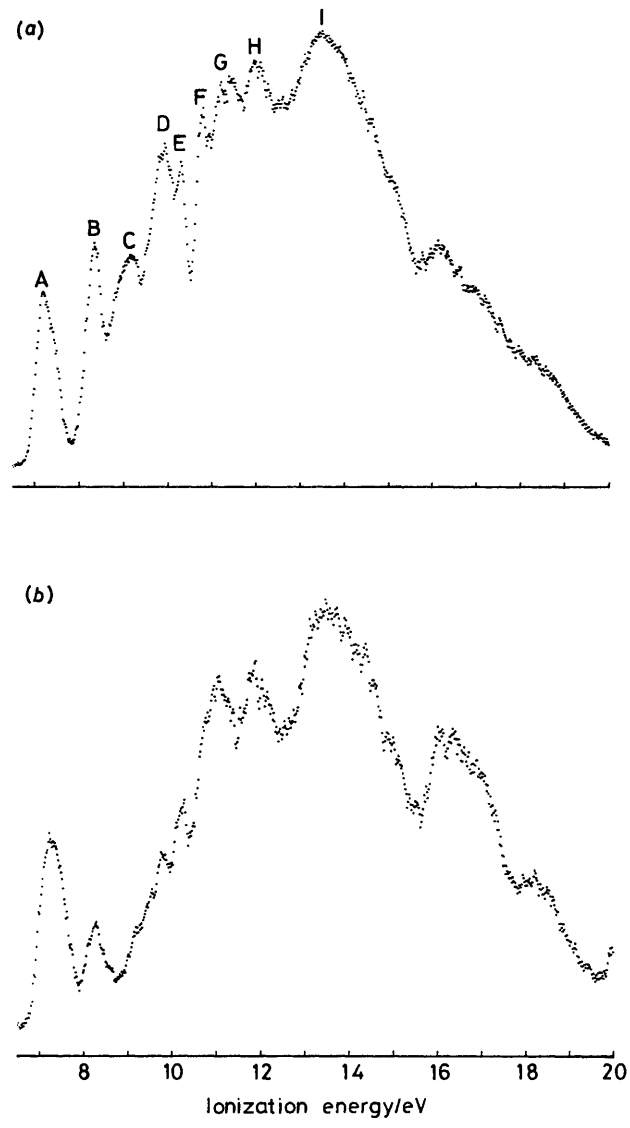

Figure 3. He I (*a*) and He II (*b*) p.e. spectra of $[Ni(dtp)_2]$

Computational Details.—The use of pseudopotentials to simulate atomic core electrons and thus to reduce the computer time associated with *ab initio* m.o. calculations is well known and they are now being integrated into standard *ab initio* codes. The calculations reported here use such pseudopotentials. To investigate whether different implementations of the atomic pseudopotentials lead to significantly different results, we have carried out SCF calculations on one of the molecules studied here, $[Pd(dtp)_2]$, using two different representations of the pseudopotentials.

(*i*) The first, denoted PS1, uses a semi-local representation of the pseudopotentials, with the parameters of Daudey *et al.*[14] The valence basis was of double-zeta quality, as described elsewhere.[12,15] These potentials were implemented by the program PSHONDO,[16] a modified version of HONDO.

(*ii*) The second representation of the pseudopotentials, denoted PS2, is a non-local one,[17] of particular value in geometry optimization studies, and is obtained for sulphur, phosphorus, and the metal atoms by transforming the semi-local potentials of Hay and Wadt.[18] For oxygen, the non-local potential was obtained from Daudey.[19] The valence basis sets were of double-zeta quality and were taken from Hay and

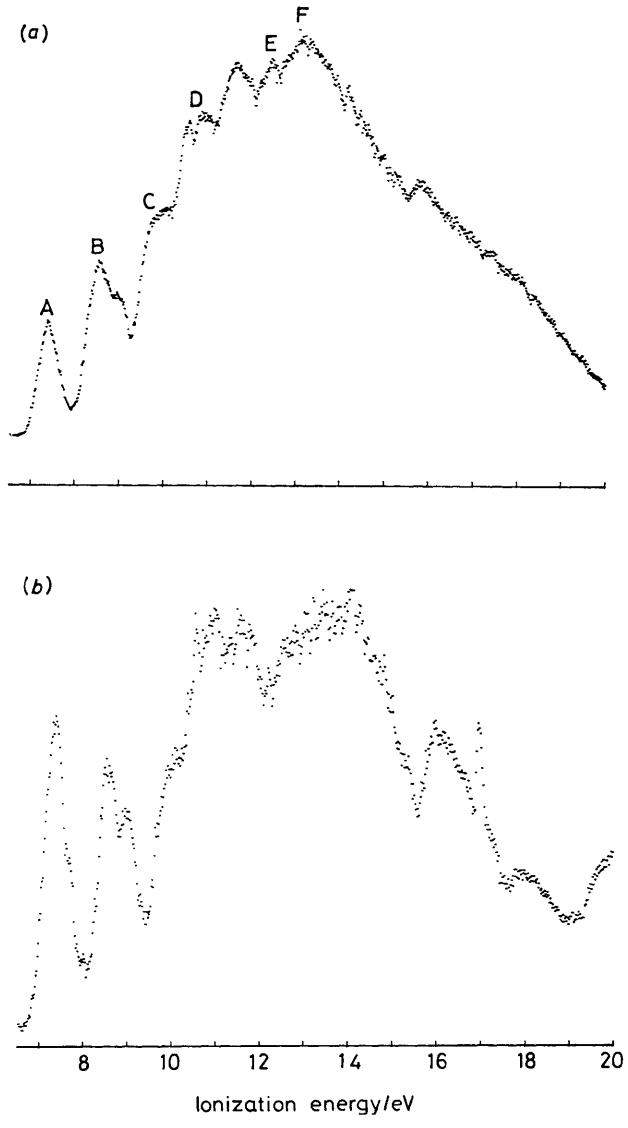

Figure 4. He I (*a*) and He II (*b*) p.e. spectra of $[Pt(dtp)_2]$

Table 1. *Ab initio* eigenvalues and population analysis of the outermost m.o.s of dtp^-

		% Population				
M.o.	Eigenvalue/eV	S	P	O	H	M.o. type
$4b_1$	−3.66	97	3	—	—	n_-
$2a_2$	−4.33	99	—	1	—	π_-
$6a_1$	−5.48	91	7	2	—	n_+
$4b_2$	−5.58	78	15	7	—	π_+
$3b_1$	−6.88	56	25	19	—	σ
$5a_1$	−9.66	44	23	33	—	σ
$1a_2$	−11.24	1	—	99	—	$n(O_{2p_x})$
$3b_2$	−12.54	2	11	82	5	$n(O_{2p_z})$

Wadt[18] for sulphur, phosphorus, and the metal atoms, and for oxygen was constructed from the all-electron basis of Dunning,[20] omitting the core functions. In calculations on $[Pd(dtp)_2]$, *d*-polarization functions having exponents 0.65 and 0.55 respectively were used for the sulphur and phosphorus atoms. These non-local potentials were implemented by the program GAMESS.[21]

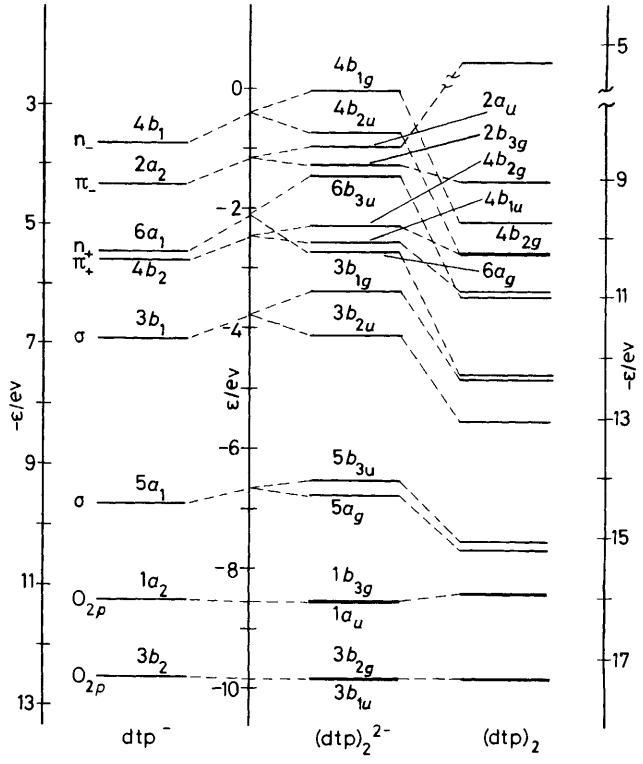

Figure 5. Correlation diagram between orbital eigenvalues of dtp^-, $(dtp)_2^{2-}$, and $(dtp)_2$

For $[Pt(dtp)_2]$, SCF calculations were carried out using the potentials PS1. Here the pseudopotentials[22] for the platinum atom included the major relativistic (mass and Darwin) corrections.[23,*] For $[Pd(dtp)_2]$ and $[Ni(dtp)_2]$, calculations at the SCF level were carried out using the potentials PS2. For these two molecules, calculations of the molecular i.e.s which included both relaxation and correlation effects were carried out by the Tamm–Dancoff method. These calculations included the lowest 19 and 20 virtual orbitals respectively.

Geometrical parameters used in the present calculations were adapted using *X*-ray data for the $[Ni(dtp)_2]$ complex,[5] since the same structures have been found along the series.[5b] Therefore a M–S distance of 2.32 Å was deduced from average Pd–S and Pt–S distances found in other square-planar MS_4 complexes.[26] The calculations were carried out on model compounds of D_{2h} symmetry where the ethyl groups (R) have been replaced by hydrogen atoms (Figure 1). The axis system adopted is shown in Figure 1.

Experimental Results

The He I and the He II p.e. spectra of the three complexes are shown in Figures 2—4. The spectra of all three complexes show three low-energy bands (A—C) whose relative intensities change on going from He I to He II ionizing radiation. We note that the intensity of the first band (A) increases relative to B and C, this increase being particularly marked for the nickel complex.

* The effects of spin–orbit coupling have not been explicitly taken into account since the absence of degenerate levels prevents (Kramer's theorem) the observation of ion states more than ground-state m.o.s. Furthermore, it is well known that off-diagonal mixing in the corresponding double group due to the so-called 'induced or indirect spin–orbit effect'[24] is of a minor relevance in square-planar platinum(II) complexes.[25]

Table 2. *Ab initio* eigenvalue and population analysis of the outermost m.o.s of the $(dtp)_2^{2-}$ cluster

		% Population				
M.o.	Eigenvalue*/eV	S	P	O	H	Character
$4b_{1g}$	−0.10 (−9.76)	95 (98)	4 (1)	1 (1)	—	n_-
$4b_{2u}$	−0.73 (−10.32)	95 (97)	5 (3)	—	—	n_-
$2a_u$	−0.97 (−5.32)	99 (99)	—	1 (1)	—	π_-
$2b_{3g}$	−1.28 (−9.10)	99 (99)	—	1 (1)	—	π_-
$6b_{3u}$	−1.47 (−11.01)	88 (89)	10 (6)	2 (5)	—	n_+
$4b_{2g}$	−2.31 (−10.28)	76 (75)	18 (15)	6 (10)	—	π_+
$4b_{1u}$	−2.59 (−10.96)	77 (77)	17 (14)	6 (9)	—	π_+
$6a_g$	−2.73 (−12.30)	91 (91)	7 (5)	2 (4)	—	n_+
$3b_{1g}$	−3.39 (−12.36)	55 (54)	29 (21)	16 (25)	—	σ
$3b_{2u}$	−4.11 (−13.09)	56 (54)	25 (17)	19 (29)	—	σ
$5b_{3u}$	−6.53 (−15.11)	49 (37)	25 (18)	26 (45)	—	σ
$5a_g$	−6.77 (−15.25)	45 (33)	25 (16)	30 (51)	—	σ
$1b_{3g}$	−8.55 (−15.99)	1 (1)	—	99 (99)	—	$n(O_{2p_y})$
$1a_u$	−8.56 (−15.98)	1 (1)	—	99 (99)	—	$n(O_{2p_y})$
$3b_{2g}$	−9.84 (−17.36)	1 (2)	11 (13)	83 (80)	5 (5)	$n(O_{2p_x})$
$3b_{1u}$	−9.84 (−17.37)	1 (2)	11 (13)	83 (80)	5 (5)	$n(O_{2p_x})$

Orbital population*	S	P	O	H
s	1.88 (1.92)	1.44 (1.38)	1.77 (1.79)	0.59 (0.56)
p_σ	2.70 (2.81)	2.30 (2.14)	4.93 (4.86)	
p_π	1.79 (1.30)	0.94 (1.02)		
Atomic charge*	−0.37 (−0.03)	+0.31 (+0.46)	−0.70 (−0.64)	+0.41 (+0.44)

Overlap population*	S–P	P–O	O–H
	0.86 (0.70)	−0.13 (0.02)	0.60 (0.60)

* Values for $(dtp)_2$ are given in parentheses.

Computational Results

Bonding in $[M(dtp)_2]$.—Before discussing the electronic structure of the $[M(dtp)_2]$ complexes it is useful to study the nature of the higher valence m.o.s of the dtp^- anion ligand that are involved in the metal–ligand interactions. The results of a m.o. calculation using the pseudopotentials PS1 are shown in Table 1. The higher m.o.s can be described in terms of a combination of the two in-plane sulphur lone pairs $[n_+(a_1), n_-(b_1)]$ and of the two higher lying m.o.s of π symmetry $[\pi_+(b_2), \pi_-(a_2)]$. The latter m.o.s involve combinations of the two out-of-plane sulphur lone pairs.

In a $(dtp)_2^{2-}$ cluster in which the separation of the ligands is comparable to that in the complexes, each of the m.o.s of dtp^- give rise to two m.o.s (of g and u symmetries in D_{2h}) split due to interligand interaction. Such splitting is, as expected, found to be larger for the in-plane than for the out-of-plane orbitals. The results of the calculations are shown in Table 2 and Figure 5 which has been drawn to line up the energies of the O_{2p}-based m.o.s ($3b_{1u}$, $3b_{2g}$). In this figure we also show the energies of the m.o.s of the neutral species $(dtp)_2$.

We turn now to a description of the bonding in $[Pd(dtp)_2]$. The results of the SCF calculations on this molecule are summarized in Tables 3 and 4. In Table 3 a comparison of the eigenvalues using both PS1 and PS2 is made. It can be seen that both calculations yield similar values. The composition of the individual m.o.s is also very similar in both calculations. We are thus confident that the conclusions to be drawn from our calculations are essentially independent of the pseudopotential used.

The m.o. population analysis (Table 3) shows that the metal $4d$ orbitals of π symmetry (d_{xz}, d_{yz}) are admixed only to a minor extent with the ligand m.o.s, so that both the $4b_{2g}$ and $2b_{3g}$ m.o.s of the complex (Table 3) possess almost pure metal d character. There are however relevant interactions between metal orbitals of σ symmetry, $4d_{x^2-y^2}$, $4d_{z^2}$, and the $5a_g$ and $6a_g$ ligand m.o.s respectively. The interaction involving the $4d_{x^2-y^2}$ orbital results in the $5a_g$ and $7a_g$ m.o.s of the complex (Table 3) which represent a pair of Pd–S bonding and antibonding m.o.s (Figure 6). In the case of the $4d_{z^2}$ orbital, both the resulting $6a_g$ and $8a_g$ m.o.s possess Pd–S bonding character due to the stabilizing interactions with the empty metal $5s$ orbital in the $8a_g$ m.o. (Figure 6). However, the major metal–ligand bonding interaction involves the empty Pd $4d_{xy}$ orbital and the $4b_{1g}$ (n_-) ligand m.o. Thus, the resulting $3b_{1g}$ m.o. of $[Pd(dtp)_2]$ has the greatest Pd–S overlap population and the greatest change in the charge distribution of the $(dtp)_2^{2-}$ cluster on complex formation is a decrease in the population of the ligand p_σ orbitals (Table 4).

Turning to $[Pt(dtp)_2]$, we note a close similarity of population data (Table 5) for m.o.s having no metal contribution to the corresponding values found for $[Pd(dtp)_2]$. By contrast, differences are found in the case of those m.o.s which are admixed with metal orbitals of a_g, b_{2g}, and b_{3g} symmetries. In particular, metal $5d$ subshells of π symmetry are admixed to a larger extent than in $[Pd(dtp)_2]$, with the $3b_{3g}$ (π_-) and $5b_{2g}$ (π_+) m.o.s acquiring stronger Pt–S antibonding character (Table 5). Furthermore, the $7a_g$ and $8a_g$ m.o.s possess greater metal d character. This is at variance with $[Pd(dtp)_2]$, where the same m.o.s were rather admixed with more internal ligand $5a_g$ and $6a_g$ orbitals. Finally, we note in $[Pt(dtp)_2]$ a larger metal $6s$ contribution to $6a_g$ and $8a_g$ m.o.s, which increases their bonding character.

For $[Ni(dtp)_2]$, the ligand-localized m.o.s have a similar energy to those of the palladium and platinum complexes (Table 6). However, the degree of localization of the m.o.s is greater than that found in the palladium and platinum

Table 3. *Ab initio* eigenvalues[a] and population analysis of the outermost m.o.s of $[Pd(dtp)_2]$

		% Population								
		Pd							Overlap population	Dominant
M.o.	Eigenvalue/eV	4*d*	5*s*	5*p*	S[b]	P	O	H	Pd–S	character
$3b_{3g}$	−10.04 (−9.97)	12	—	—	87	—	1	—	−0.040	π_-, d_{yz}
$4b_{2u}$	−10.09 (−9.64)	—	—	3	95	2	—	—	0.028	n_-
$2a_u$	−10.36 (−10.34)	—	—	—	98	—	2	—	0.000	π_-
$5b_{2g}$	−10.55 (−10.58)	17	—	—	68	8	7	—	−0.042	π_+, d_{xz}
$6b_{3u}$	−11.10 (−10.51)	—	—	6	83 (2)	4	5	—	0.054	n_+
$8a_g$	−11.27 (−11.31)	42	10	—	44	3	1	—	0.024	d_{z^2}, n_+
$4b_{1u}$	−11.78 (−11.81)	—	—	1	79 (1)	8	11	—	0.010	π_+
$4b_{1g}$	−12.11 (−11.63)	7	—	—	68 (1)	13	11	—	0.006	σ
$3b_{2u}$	−13.39 (−12.84)	—	—	1	50 (1)	14	34	—	0.014	σ
$7a_g$	−13.91 (−13.69)	51	—	—	19	11	19	—	−0.016	$d_{x^2-y^2}$, σ
$3b_{1g}$	−13.95 (−14.23)	29	—	—	42 (2)	4	23	—	0.062	n_-, d_{xy}
$2b_{3g}$	−14.46 (−14.38)	87	—	—	12	—	1	—	0.032	d_{yz}, π_-
$4b_{2g}$	−14.78 (−14.84)	80	—	—	11 (1)	1	7	—	0.035	d_{xz}, π_+
$6a_g$	−14.84 (−14.54)	49	—	—	36 (1)	2	12	—	0.036	d_{z^2}, n_+
$5b_{3u}$	−15.15 (−15.17)	—	—	—	35 (1)	15	49	—	0.000	σ
$1a_u$	−15.85 (−16.38)	—	—	—	2	—	98	—	0.000	$n(O_{2p_y})$
$1b_{3g}$	−15.86 (−16.39)	—	—	—	2	—	98	—	0.000	$n(O_{2p_y})$
$5a_g$	−16.54 (−16.37)	46	—	—	16	3	35	—	0.028	$\sigma, d_{x^2-y^2}$
$3b_{1u}$	−17.21 (−17.15)	—	—	—	4	12	79	5	0.000	$n(O_{2p_x})$
$3b_{2g}$	−17.24 (−17.16)	2	—	—	4	12	76	6	0.002	$n(O_{2p_x})$

[a] The results in this table are from the calculation using PS1, except for the eigenvalues in parentheses which are from the calculation using PS2. [b] Population percentages of sulphur 3*d* atomic orbitals (a.o.s) are in parentheses.

Table 4. Atomic charges and orbital and overlap populations of $[Pd(dtp)_2]$ and $[Pt(dtp)_2]$ [values for the $(dtp)_2^{2-}$ cluster are in parentheses]

		(dtp)$_2$			
Orbital population	Pd	S	P	O	H
s	0.32	1.85 (1.88)	1.27 (1.44)	1.80 (1.77)	0.56 (0.59)
p_σ	0.35	2.58 (2.70)	1.96 (2.30)	4.87 (4.93)	
p_π	0.03	1.84 (1.79)	0.85 (0.95)		
d_σ x^2-y^2	1.96	0.01			
d_σ z^2	1.95	0.01			
d_σ xy	0.88	0.05			
d_π xz	1.99	0.01			
d_π yz	1.99	0.01			
Atomic charges	+0.52	−0.36 (−0.37)	+0.91 (+0.31)	−0.66 (−0.70)	+0.44 (+0.41)
Overlap population	Pd–S	S–P	P–O	O–H	
σ	0.42	0.78 (0.86)	0.23 (−0.13)	0.57 (0.60)	
π	−0.01				
	Pt	S	P	O	H
s	0.87	1.84	1.28	1.80	0.55
p_σ	0.07	2.53	1.91	4.87	
p_π	0.03	1.85	0.84		
d_σ x^2-y^2	1.95	0.01			
d_σ z^2	1.92	0.01			
d_σ xy	0.99	0.05			
d_π xz	1.99	0.01			
d_π yz	1.98	0.01			
Atomic charges	+0.20	−0.32	+0.98	−0.67	+0.45
Overlap population	Pd–S	S–P	P–O	O–H	
σ	0.46	0.74	0.23	0.57	
π	−0.11				

complexes, with predominantly metal m.o.s being considerably more tightly bound, in line with the corresponding atomic ionization energies. The atomic charges and orbital populations (Table 7) are similar to those in the other two complexes, especially as far as the population of the partially occupied d_{xy} orbital is concerned.

Interpretation of Photoelectron Spectra

$[Pd(dtp)_2]$.—In Table 8 we show the valence i.e.s of $[Pd(dtp)_2]$ calculated using the Tamm–Dancoff method. The results are shown for three different atomic basis sets. The first has no polarization functions on the ligands, the second has a *d* function on sulphur, and the third a *d* function on both sulphur

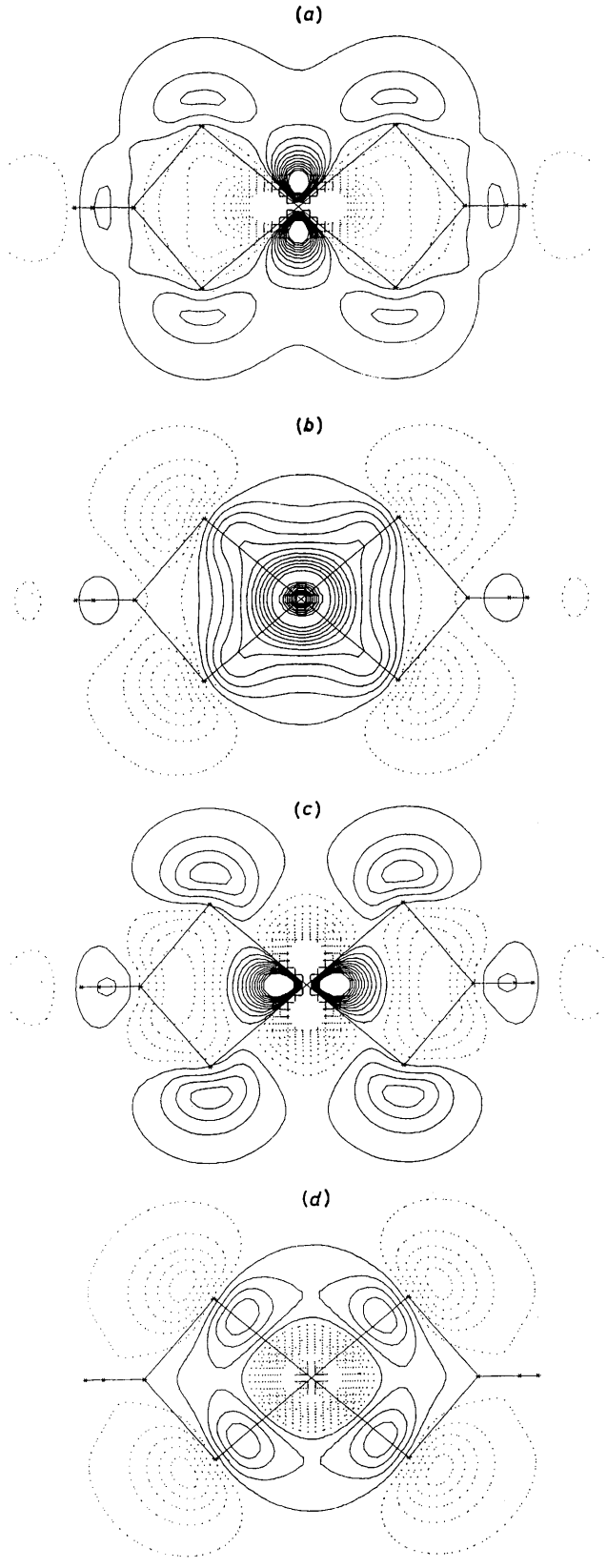

Figure 6. Wavefunction contour plots of $[Pd(dtp)_2]$ for the $5a_g$ (*a*), $6a_g$ (*b*), $7a_g$ (*c*), and $8a_g$ (*d*) m.o.s in the *xy* plane. Each set of contours is drawn in a frame of 10 × 10 a.u. (1 a.u. = 0.052 917 nm) and the stars indicate projections of each atom on the contour plane. The interval between successive contours is $0.017\ e^{\frac{1}{2}}$ a.u.$^{-\frac{3}{2}}$. The point lines refer to the negative part of the wavefunction

and phosphorus. It can be seen that the introduction of the polarization functions has little effect on the calculated i.e.s and certainly does not affect the assignment of the p.e. spectrum. We note, however, that larger bases improve the reproduction of the experimental i.e.s to a small extent.

The measured p.e. spectrum (Figure 2) shows definite intensity changes on going from He I to He II ionizing radiation. Bands A and B increase in intensity relative to C. Moreover, band B looses its shoulder in the He II spectrum, and its total intensity increase appears somewhat smaller than found for band A. The shoulders (D and E) also increase in intensity relative to band C in the He II spectrum.

Turning to the calculated i.e.s shown in Table 8, we see from a comparison with the orbital eigenvalues (Table 3) that the order of the i.e.s is not *drastically* changed from that given by Koopmans' theorem. The well known effect of greater orbital relaxation accompanying ionization from metal- compared to ligand-localized orbitals is seen, but the effect is considerably less than that found in complexes containing first-row transition metals, such as bis-π(allyl)nickel.[9] These values are arranged in well separated groups that, given an almost uniform shift (~1 eV), nicely fit the main spectral features up to 13—14 eV. Moreover the energy dispersion within each group agrees well with experimental bandwidths. We note, however, that the lack of ethyl groups in the calculations prevents a definite assignment of all features beyond 12 eV. Therefore, band A is assigned to ionization from the $4b_{2u}$ and $3b_{3g}$ m.o.s. The second of these involves the Pd $4d_{yz}$ orbital so that some intensity increase in He II compared to that of pure ligand m.o.s is to be expected. The second band (B) is assigned to the four m.o.s $5b_{2g}$, $8a_g$, $2a_u$, and $6b_{3u}$. The $5b_{2g}$ and $8a_g$ m.o.s have metal *d* character, which is near to 50% for the latter orbital. The loss of the low-energy shoulder of band B in the He II spectrum is consistent with the $8a_g$ i.e. being somewhat larger than that of the $5b_{2g}$. We would however note that this assignment of bands A and B is open to some doubt in view of the somewhat *smaller* intensity change in He II found for band B compared to band A, and the rather *larger* Pd 4*d* population of the $8a_g$ compared to the $3b_{3g}$ m.o. The decrease in intensity of band C, compared to bands A and B, on going from He I to He II radiation is in line with our assignment of band C to ionization from the predominantly ligand orbitals, $4b_{1g}$ and $4b_{1u}$. We assign the shoulders (D, E) on the rapidly rising spectrum to ionization from the strongly metal $7a_g$ and $2b_{3g}$ m.o.s. We have already noted that band C (due to l.b. ionizations) decreases in intensity compared to these shoulders in the He II spectrum. We assign the broad band F and G to two groups of orbitals (Table 8) separated by ~1.5 eV, the first group containing two m.o.s having considerable metal character ($4b_{2g}$ and $6a_g$), and the second group containing one such m.o. ($5a_g$).

$[Ni(dtp)_2]$.—The valence i.e.s of $[Ni(dtp)_2]$ calculated by the Tamm–Dancoff method are shown in Table 9. In view of the small effect shown by ligand-polarization functions on the calculated i.e.s of $[Pd(dtp)_2]$, no such polarization functions were used in the $[Ni(dtp)_2]$ calculation. When compared with the i.e.s from Koopmans' theorem, the values shown in Table 9 exhibit considerable changes. For example, when correlation and relaxation effects are considered the first i.e. corresponds to ionization from the mainly metal $6a_g$ m.o., which is one of the more strongly bound m.o.s at the SCF level (Table 6). An interpretation of the p.e. spectrum in terms of Koopmans' theorem i.e.s is clearly not possible. However, the i.e.s calculated by the present method do lead to a consistent interpretation of the p.e. spectrum shown in Figure 3. The most dramatic change in the intensity profile of this spectrum on going from He I to He II radiation is a considerable increase in the intensity of the first band (A) relative to that of the next three (B—D).

Table 5. *Ab initio* eigenvalues and population analysis of the outermost m.o.s of $[Pd(dtp)_2]$

		% Population								
		Pt							Overlap population	Dominant
M.o.	Eigenvalue/eV	5*d*	6*s*	6*p*	S*	P	O	H	Pt–S	character
$3b_{3g}$	−9.62	25	—	—	74	—	1	—	−0.096	π_-, d_{yz}
$5b_{2g}$	−9.94	31	—	—	57	7	5	—	−0.092	π_+, d_{xz}
$4b_{2u}$	−10.50	—	—	1	98	1	—	—	0.006	n_-
$2a_u$	−10.56	—	—	—	98	—	2	—	0.000	π_-
$8a_g$	−10.77	69	19	—	12	—	—	—	0.020	d_{z^2}, n_+
$6b_{3u}$	−11.50	—	—	—	87 (2)	5	5	1	0.000	n_+
$4b_{1u}$	−11.96	—	—	1	81	7	11	—	0.008	π_+
$4b_{1g}$	−12.32	5	—	—	68 (1)	14	12	—	0.006	σ
$7a_g$	−12.77	67	—	—	13 (1)	9	10	—	−0.032	$d_{x^2-y^2}$, σ
$3b_{2u}$	−13.56	—	—	—	52 (2)	13	33	—	0.000	σ
$2b_{3g}$	−13.59	74	—	—	25	—	1	—	0.060	d_{yz}, π_-
$4b_{2g}$	−14.10	66	—	—	23 (1)	1	9	—	0.064	d_{xz}, π_+
$3b_{1g}$	−14.37	30	—	—	40 (2)	3	25	—	0.058	n_-, d_{xy}
$6a_g$	−15.01	20	10	—	47 (1)	2	20	—	0.056	d_{z^2}, n_+
$5b_{3u}$	−15.29	—	—	—	35 (1)	14	50	—	0.000	σ
$1a_u$	−15.91	—	—	—	2	—	98	—	0.000	$n(O_{2p_y})$
$1b_{3g}$	−15.92	—	—	—	2	—	98	—	0.000	$n(O_{2p_y})$
$5a_g$	−16.41	30	1	—	24 (1)	5	38	1	0.028	$\sigma, d_{x^2-y^2}$
$3b_{1u}$	−17.27	—	—	—	4	12	79	5	0.000	$n(O_{2p_x})$
$3b_{2g}$	−17.31	—	—	—	3	12	80	5	0.000	$n(O_{2p_x})$

* Population percentages of sulphur 3*d* a.o.s are in parentheses.

Table 6. *Ab initio* eigenvalues and population analysis of the outermost m.o.s of $[Ni(dtp)_2]$

		% Population							
		Ni							
M.o.	Eigenvalue/eV	3*d*	4*s*	4*p*	S	P	O	H	Dominant character
$4b_{2u}$	−10.14					97	2		n_-
$2a_u$	−10.42					99		1	π_-
$6b_{3u}$	−10.75				11	77	6	8	n_+
$3b_{3g}$	−10.84	3				96		1	π_-
$4b_{1g}$	−11.04	16				74	6	4	σ
$5b_{2g}$	−11.55	5				74	14	8	π_+
$4b_{1u}$	−12.19				4	76	12	8	π_+
$3b_{2u}$	−12.80				8	49	15	27	σ
$3b_{1g}$	−12.87	21				43	14	21	σ, d_{xy}
$8a_g$	−13.20	16	18			59	5	3	n_+, d_{z^2}
$5b_{3u}$	−15.10					40	16	43	σ
$7a_g$	−15.26	7				29	12	52	σ
$6a_g$	−16.04	75				19		6	d_{z^2}
$2b_{3g}$	−16.53	2						98	$n(O_{2p_y})$
$1a_u$	−16.53					1		99	$n(O_{2p_y})$
$4b_{2g}$	−17.01	50					6	46	1 $d_{xz}, n(O_{2p_x})$
$1b_{3g}$	−17.08	96				3		1	d_{yz}
$3b_{1u}$	−17.32				3	3	10	86	3 $n(O_{2p_x})$
$3b_{2g}$	−17.56	46				5	7	39	2 $d_{xz}, n(O_{2p_x})$
$1b_{1g}$	−18.33	2				13	17	68	$n(O_{2p_y})$
$4b_{3u}$	−18.38				1	33	17	47	1 σ
$2b_{2u}$	−18.47				3	15	18	66	$n(O_{2p_y})$
$5a_g$	−18.65	56	2			7	7	27	1 $d_{x^2-y^2}$
$4a_g$	−19.72	46	1			30	11	11	1 $d_{x^2-y^2}$

Table 7. Atomic charges and orbital populations of $[Ni(dtp)_2]$

		$(dtp)_2$			
Orbital population	Ni	S	P	O	H
s	0.30	1.96	1.37	1.99	0.55
p_σ	0.5	2.43	1.68	3.63	
p_π	0.1	1.80	0.73	1.31	
d_σ x^2-y^2	2.02				
d_σ z^2	2.02				
d_π xy	0.84				
d_π xz	2.02				
d_π yz	2.01				
Atomic charge	+0.24	−0.19	+1.22	−0.93	+0.45

Our calculations do lead to an assignment consistent with this observed pattern. Thus, band A is assigned to ionization from the $6a_g$ and $3b_{3g}$ m.o.s, the former m.o. being calculated to have 75% nickel 3*d* character. Bands B and C are assigned to ionization from m.o.s which have less than 10% metal character: B is associated with the $5b_{2g}$ and $4b_{2u}$ and C with the $2a_u$ and $6b_{3u}$ m.o.s. Band D, which shows some increase in intensity in the He II spectrum, is assigned to ionization from the $4b_{1g}$ m.o. calculated to have 16% nickel 3*d* character. Band E which is definitely more intense in He II is assigned to ionization from the $1b_{3g}$ and $5a_g$ m.o.s, both having considerable metal character. The remaining ionizations, except that involving the $4b_{2g}$ m.o., are from m.o.s of predominantly ligand character. Our remaining assignment shown in Table 9 is thus similar to that for the corresponding region of the p.e. spectrum of the palladium complex.

$[Pt(dtp)_2]$.—The p.e. spectra of $[Pt(dtp)_2]$ (Figure 4) show a close resemblance to that of the palladium complex (Figure 2), with two low-energy bands (A, B) and a pronounced shoulder (C). The relative intensity of the first band (A) increases, relative to that of bands B and C, in the He II spectrum. Compared to the spectrum of $[Pd(dtp)_2]$ the shoulder on band B is to high rather than to low i.e., and this shoulder is evident in both He I and He II spectra. The only calculation on $[Pt(dtp)_2]$ that we have carried out is at the SCF level and is shown in Table 5. We have already noted that for $[Pd(dtp)_2]$, in contrast to $[Ni(dtp)_2]$, the ordering of the i.e.s must be close to that given by Koopmans' theorem. We would expect a similar situation to hold for $[Pt(dtp)_2]$

Table 8. Ionization energies (eV) of $[Pd(dtp)_2]$ calculated using the Tamm–Dancoff method

Orbital	Ionization energy: Basis I	Basis II[a]	Basis III[b]	Assignment of p.e. spectrum[c]
$4b_{2u}$	8.66	8.62	8.29	A (8.0)
$3b_{3g}$	8.66	8.70	8.40	
$5b_{2g}$	9.25	9.07	8.80	B (8.50, 8.72)
$8a_g$	9.39	9.26	9.02	
$2a_u$	9.49	9.35	9.04	
$6b_{3u}$	9.86	9.79	9.71	
$4b_{1g}$	10.62	10.85	10.62	C (9.30, 9.60)
$4b_{1u}$	11.02	10.85	10.63	
$7a_g$	11.19	11.11	10.74	D (10.2)
$2b_{3g}$	11.64	11.46	11.21	E (10.7)
$3b_{2u}$	12.12	12.25	12.11	F (11—12.5)
$4b_{2g}$	12.48	12.26	11.99	
$6a_g$	12.77	12.68	12.47	
$3b_{1g}$	13.04	12.95	12.71	
$5b_{3u}$	14.21	14.28	14.22	G (~13)
$5a_g$	14.82	14.87	15.03	
$1b_{3g}$	15.02	14.94	15.08	
$1a_u$	15.03	14.95	15.08	

[a] *d* Polarization function on sulphur. [b] *d* Polarization function on sulphur + phosphorus. [c] See Figure 2; the values in parentheses are the measured i.e.s.

Table 9. Ionization energies (eV) of $[Ni(dtp)_2]$ calculated using the Tamm–Dancoff method

Orbital	Ionization energy	Assignment of p.e. spectrum*
$6a_g$	8.55	A (7.20)
$3b_{3g}$	8.66	
$5b_{2g}$	8.91	B (8.30)
$4b_{2u}$	9.09	
$2a_u$	9.49	C (9.16)
$6b_{3u}$	9.94	
$4b_{1g}$	10.26	D (9.84)
$5a_g$	10.67	E (10.28)
$1b_{3g}$	10.83	
$4b_{1u}$	11.24	F (10.73)
$4b_{2g}$	11.53	
$3b_{1g}$	12.07	G (11.35)
$3b_{2u}$	12.15	
$8a_g$	12.86	H (11.94)
$5b_{3u}$	14.10	I (13.40)
$7a_g$	14.65	
$1a_u$	15.00	
$2b_{3g}$	15.01	

* See Figure 3; the values in parentheses are the measured i.e.s.

and we therefore use the eigenvalues for $[Pt(dtp)_2]$ (Table 5) and for $[Pd(dtp)_2]$ (Table 3) together with our assignment of the p.e. spectrum of $[Pd(dtp)_2]$ (Table 8) to assign the spectrum of $[Pt(dtp)_2]$. We note that in the platinum complex the $8a_g$ m.o. has considerably more metal *d* character than in the palladium complex, which will probably lead to greater electron relaxation upon ionization. We therefore assign $8a_g$ and $3b_{3g}$ ionization to band A, $5b_{2g}$, $4b_{2u}$, $2a_u$, and $6b_{3u}$ to band B, and $4b_{1u}$ and $4b_{1g}$ to band C. Thus, in contrast to our assignment of the p.e. spectrum of $[Pd(dtp)_2]$, we assign no orbital having a large metal *d* component to the band B, so that the profile of this band is expected to be largely unchanged in the He I and He II spectra, which is observed experimentally (Figure 4).

Conclusion

This paper is a part of a comprehensive study on the electronic structure of square-planar complexes, and presents a case study of ligands containing sulphur chromophores.

In accordance with studies on other square-planar complexes containing either O_4 or N_4 chromophores,[12,15] there is evidence that, also in the S_4 case, almost all the upper-filled m.o.s of the ligand cluster are involved in the metal–ligand bonding. In particular, in addition to outermost m.o.s related to σ and π lone pairs of heteroatoms, interactions also involve more internal delocalized l.b. m.o.s. The present theoretical and p.e. data fit nicely to a bonding model in which metal *d* subshells lie intermediate in energy among the ligand m.o.s.

In these complexes the dominant interactions are σ in character and involve both filled ($d_{x^2-y^2}$, d_{z^2}) and empty (d_{xy}, *s*) metal orbitals. π Interactions are of a minor relevance and metal $d_{xz,yz}$ orbitals are almost non-bonding in character. The ordering of the conventional metal subshells $d_{xz} \approx d_{yz} < d_{x^2-y^2} < d_{z^2} \ll d_{xy}$ found for the platinum and palladium complexes suggests classification of the dtp ligand as a classical strong σ-donor, weak π-acceptor ligand.[2,7] As expected, the metal–ligand covalency, as measured by the metal d_{xy} populations, is Pt > Pd > Ni, reflecting the degree of ligand-to-metal σ donation.

Despite the apparently simple patterns of the reported spectra, no simple qualitative interpretation is practicable. The overall p.e. data, in fact, do not fit any classical model by which the four occupied metal *d* subshells represent the outermost filled m.o.s, as supposed in an earlier study.[4]

The pseudopotential *ab initio* method, in conjunction with the Tamm–Dancoff method, has proven capable of providing a suitable rationale for the p.e. data, although the accuracy of the calculations may not be high enough to provide an unquestionable assignment of the p.e. spectra.

The energy sequence of states produced upon ionization is largely dominated by reorganization effects in the ion, although correlation effects are also of relevance in arriving at a correct ordering of the states. Since the relaxation energy associated with a particular m.o. is roughly proportional to the contribution of the metal *d* orbitals, the greater degree of *d*-electron localization in the nickel complex gives rise to larger deviations from Koopmans' theorem than is found in the palladium and platinum complexes. This means that the simple comparison of the i.e.s of the three complexes does not afford a real picture of differences in the bonding.

Acknowledgements

The authors thank the Consiglio Nazionale delle Ricerche (C.N.R., Rome, Italy), the Ministero della Pubblica Istruzione (M.P.I., Rome, Italy), and the S.E.R.C. for financial support. We thank Professor W. von Niessen for use of his Tamm–Dancoff program.

References

1 R. Eisenberg, *Prog. Inorg. Chem.*, 1970, **12**, 295; D. Coucouvanis, *ibid.*, 1970, **11**, 233; D. Coucouvanis, *ibid.*, 1979, **26**, 301; G. Granozzi, A. Vittadini, L. Sindellari, and D. Ajò, *Inorg. Chem.*, 1984, **23**, 702; S. Alvarez, R. Vicente, and R. Hoffmann, *J. Am. Chem. Soc.*, 1985, **107**, 6253; M. P. Sigas and C. A. Tsipis, *Inorg. Chem.*, 1986, **25**, 1875.

2 (*a*) F. N. Tebbe and E. L. Muetterties, *Inorg. Chem.*, 1970, **9**, 629; (*b*) R. G. Cavell, W. Byers, E. D. Day, and P. M. Watkins, *ibid.*, 1972, **11**, 1598; (*c*) J. R. Wasson, G. M. Woltermann, and H. J. Stoklosa, *Fortschr. Chem. Forsch.*, 1973, **35**, 65; (*d*) R. C. Mehrotra, G. Srivastava, and B. P. S. Chauhan, *Coord. Chem. Rev.*, 1984, **55**, 207.

3 C. K. Jorgensen, *J. Inorg. Nucl. Chem.*, 1962, **24**, 1571; A. A. G. Tomlinson and C. Furlani, *Inorg. Chim. Acta*, 1969, **3**, 487; J. D. Lebedda and R. A. Palmer, *Inorg. Chem.*, 1972, **11**, 484; K. Myers and

G. Andermann, *J. Phys. Chem.*, 1973, **77**, 280; G. Ciullo and A. Sgamellotti, *Z. Phys. Chem. (Munich)*, 1976, **100**, 67; M. V. Andreocci, P. Dragoni, A. Flamini, and C. Furlani, *Inorg. Chem.*, 1978, **17**, 291.
4 J. P. Maier and D. A. Sweigart, *Inorg. Chem.*, 1976, **15**, 1989.
5 (*a*) Q. Fernando and C. D. Green, *J. Inorg. Nucl. Chem.*, 1967, **29**, 647; (*b*) J. F. McConnell and V. Kastalsky, *Acta Crystallogr.*, 1967, **22**, 853.
6 S. E. Livingstone and A. E. Mihkelson, *Inorg. Chem.*, 1970, **9**, 2545.
7 G. Cooper, J. C. Green, M. P. Payne, B. R. Dobson, and I. H. Hillier, *J. Am. Chem. Soc.*, 1987, **109**, 3836.
8 I. H. Hillier, *Pure Appl. Chem.*, 1979, **51**, 2183; A. Veillard and J. Demuynck, in 'Modern Theoretical Chemistry,' ed. H. F. Schaefer, Plenum, New York, 1977, vol. 4, p. 187.
9 D. Moncrieff, I. H. Hillier, V. R. Saunders, and W. von Niessen, *Inorg. Chem.*, 1985, **24**, 4247.
10 S. Smith, D. A. Taylor, I. H. Hillier, M. A. Vincent, M. F. Guest, A. A. MacDowell, W. von Niessen, and D. S. Urch, *J. Chem. Soc., Faraday Trans. 2*, 1988, 209.
11 N. A. Burton, I. H. Hillier, M. F. Guest, and J. Kendrick, *Chem. Phys. Lett.*, 1989, **155**, 195.
12 S. Di Bella, I. Fragala, and G. Granozzi, *Inorg. Chem.*, 1986, **25**, 3997.
13 J. Schirmer and L. S. Cederbaum, *J. Phys. B*, 1978, **11**, 1889; J. Schirmer, L. S. Cederbaum, and O. Walter, *Phys. Rev.*, 1983, **28**, 1237.
14 'Molecular *ab initio* Calculations using Pseudopotentials,' Technical Report, Laboratoire de Physique Quantique, Toulouse, 1981; J. P. Daudey, G. Jeung, M. E. Ruiz, and O. Novaro, *Mol. Phys.*, 1982, **46**, 67.
15 S. Di Bella, M. Casarin, I. Fragala, G. Granozzi, and T. J. Marks, *Inorg. Chem.*, 1988, **27**, 3993.
16 M. Dupuis, J. Rys, and H. F. King, Pseudopotential adaptation (J. P. Daudey) of HONDO 76, Quantum Chemistry Program Exchange, 1977, vol. 11, p. 338.
17 Ph. Durant and J. C. Barthelat, *Theoret. Chim. Acta*, 1975, **38**, 283.
18 P. J. Hay and W. R. Wadt, *J. Chem. Phys.*, 1985, **82**, 270; P. J. Hay, personal communication.
19 J. P. Daudey, personal communication to J. Kendrick.
20 T. H. Dunning, *J. Chem. Phys.*, 1970, **53**, 2823.
21 M. F. Guest and J. Kendrick, GAMESS User Manual, CCP1/86/1, Daresbury Laboratory, 1986.
22 J. P. Daudey, personal communication.
23 J. C. Barthelat, M. Pelissier, and Ph. Durand, *Phys. Rev. A*, 1980, **21**, 1773.
24 P. Pyykkö, *Adv. Quantum Chem.*, 1978, **11**, 353; J. G. Snijders, E. Baerends, and P. Ros, *Mol. Phys.*, 1979, **38**, 1909.
25 See, for example, P. J. Hay, *J. Am. Chem. Soc.*, 1981, **103**, 1390; J. N. Louwen, R. Hengelmolen, D. M. Grove, A. Oskam, and R. L. DeKock, *Organometallics*, 1984, **3**, 908; J. N. Louwen, R. Hengelmolen, D. M. Grove, D. J. Stufkens, and A. Oskam, *J. Chem. Soc., Dalton Trans.*, 1986, 141.
26 R. H. Holm and H. J. O'Connor, *Prog. Inorg. Chem.*, 1971, **14**, 241.
27 A. F. Williams, 'A Theoretical Approach to Inorganic Chemistry,' Springer, Berlin, 1979, p. 81.

Received 22*nd June* 1989; *Paper* 9/02642H